Check for updates

A signal-enhanced and sensitive lateral flow aptasensor for the rapid detection of PDGF-BB

Na Cheng, [ID] [a] Yujie Liu, [be] Omar Mukama, [bd] Xiaobo Han, [b] Hualin Huang, [b] Shuai Li, [b] Peng Zhou, [a] Xuewen Lu [b] and Zhiyuan Li [ID] *[abc]

Platelet-derived growth factor BB (PDGF-BB) is a potential biomarker of tumor angiogenesis. For the first time, we developed a highly sensitive aptasensor for PDGF-BB with an enhanced test line signal by using two different gold nanoparticles (AuNPs). Herein, we describe a highly sensitive biosensor for PDGF-BB detection that combines biotinylated aptamer on a sample pad and poly thymine-Cy3-AuNP-monoclonal antibody complexes against PDGF-BB immobilized on conjugate pad A. Streptavidin (SA) and rabbit anti-mouse polyclonal antibody were also immobilized in the nitrocellulose membrane at the test and control zones, respectively. When the target PDGF-BB protein was added, it first bound the aptamer, and later the monoclonal antibody to form a biotinylated complex that was captured by SA, resulting in a visual red line on the test zone. In addition, to enhance the sensitivity, another monoclonal antibody against Cy3 was conjugated on AuNP B and immobilized on conjugate pad B to form a AuNPs (A&B)-antibody-(PDGF-BB-Cy3)-aptamer-biotin-SA complex on the test line when a loading buffer was subsequently added. This approach showed a linear response to PDGF-BB from 3 ng mL^{-1} to 300 ng mL^{-1} with a limit of detection as low as 1 ng mL^{-1} obtained in 10 minutes. Our biosensor displayed results through red lines readable by the naked eye. Interestingly, our approach has been successfully applied for real sample verification, proving its applicability for cancer monitoring and diagnosis.

1. Introduction

PDGF-BB is a significant cell factor present in serum that is considered as a potential biomarker for tumor angiogenesis due to its critical role in cell growth, division and signaling processes.[1,2] It is also involved in tumor growth and progression.[2–4] Thus, the identification and quantification of PDGF-BB is of particular interest. A number of studies have developed selective and facile detection methods for PDGF-BB cancer biomarkers,[5,6] however, these approaches mainly depended on either multistep antibody-based binding assays, such as enzyme-linked immune sorbent assay (ELISA), or nanosphere-based procedures. For instance, ELISA and traditional nanospheres require complicated procedures and large sample volumes and are expensive.[7–12] Therefore, the development of novel detection methods for PDGF-BB is imperative.

Biosensors have novel implications toward developing the macromolecular detectors.[13–18] For example, existing biosensors for PDGF-BB detection include electrochemical functionalized hybrid carbon nanofiber FET-type electrode[19] and carbon-based nanocomposites with aptamer-templated silver nanoclusters.[20] Although the direct immobilization of the nanocomposites on the electrode enhances sensitivity and selectivity, their modification process is complicated and time consuming.[21]

A number of aptamers have been identified for various organisms' whole cells and compartments (*e.g.*, thrombin, DNA polymerase) through three-dimensional, covalent binding or nucleic acid hybridization in a sequence-specific manner.[22–27] Nanomaterial-based aptamers have attracted more attention compared to other detection methods owing to their remarkable low cost, reliability, sensitivity, and efficiency.[28,29] Liu *et al.* developed lateral flow aptasensor (LFA) for the simultaneous detection of PDGF-BB and thrombin.[29] Therefore, herein, we developed a signal-enhanced and sensitive direct detection method that displays readable results to the naked eye. Our assay detected PDGF-BB using two different gold nanoparticles (AuNPs) for signal and sensitivity enhancement. This method could also be used as an alternative for apparatus-based assays to simplify the detection process, thereby displaying results through red lines readable by the naked eye.

[a]Department of Anatomy and Neurobiology, Xiangya School of Medicine, Central South University, Changsha, China. E-mail: li_zhiyuan@gibh.ac.cn

[b]Key Laboratory of Regenerative Biology, Guangdong Provincial Key Laboratory of Stem Cell and Regenerative Medicine, Guangzhou Institute of Biomedicine and Health, Chinese Academy of Sciences, Guangzhou, 510530, China

[c]GZMU-GIBH Joint School of Life Sciences, Guangzhou Medical University, Guangzhou, China

[d]Department of Biology, College of Science and Technology, University of Rwanda, Avenue de l'armée, P. O. Box: 3900, Kigali, Rwanda

[e]School of Basic Medicine, Guizhou Medical University, Guizhou, China

2. Experimental

2.1. Preparation of AuNP-antibody-DNA conjugates

AuNPs with an average diameter of 40 nm were prepared using the citrate reduction method[30,31] with slight modifications. First, 1% sodium citrate (1.4 mL) (Sigma-Aldrich, Steinheim, Germany) was added to a rapidly stirred and boiling aqueous solution (100 mL) of 1 mM HAuCl$_4$ (1 mL) (Sigma-Aldrich, Steinheim, Germany). When the solution turned red, it was left to boil for additional 10 minutes, followed by cooling to room temperature under protected conditions from the light. Finally, the prepared AuNPs were stored at 4 °C.

The AuNP-antibody complex was produced as previously described[31,32] with slight modifications. Briefly, the anti-PDGF-BB monoclonal antibody (5 µL, 1 mg mL^{-1}, Abcam, Cambridge, USA) was added to 1 mL of the AuNP A (pH 8.5) solution and shaken gently for 5 minutes. The mixture was centrifuged (1.0×10^4 rpm, 35 minutes, 10 °C) and rinsed 3 times in suspension buffer I (20 mM Na$_3$PO$_4$, 0.25% Tween-20, 10% sucrose, and 0.1% NaN$_3$). The red particles were resuspended in 100 µL suspension buffer I for further use.

The five types of functionalized poly Ts oligonucleotides (COOH-poly Ts1-Cy3, COOH-poly Ts2-Cy3, COOH-poly Ts3-Cy3, COOH-poly Ts4-Cy3, and COOH-poly Ts5-Cy3) (Table 1, Shanghai Sangon Biological Engineering Technology, Shanghai, China) were resuspended in phosphate buffer (10 mM, pH 7.0). Then, the poly Ts oligonucleotides (100 mM, 100 µL) were activated by 0.1 mg of EDC (Aladdin Chemistry Co., Ltd, Shanghai, China) and 0.1 mg of NHS (Aladdin Chemistry Co., Ltd, Shanghai, China) for 30 minutes at room temperature. To quench the EDC, 0.4 µL of 2-mercaptoethanol (20 mM, Sigma-Aldrich, Steinheim, Germany) was added. Subsequently, 5 µL the mixture was added to the AuNP A-antibody complex solution (10 times concentration, 100 µL) for 30 minutes. The freshly prepared mixture was centrifuged (1.0×10^4 rpm, 10 minutes, 4 °C) and rinsed 3 times with suspension buffer II (20 mM Na$_3$PO$_4$, 5% BSA, 0.25% Tween-20, 10% sucrose, and 0.1% NaN$_3$). The poly Ts-Cy3-AuNPs A-anti-PDGF-BB complexes were therefore stored at 4 °C for further use. Conjugate pad B was prepared similarly using AuNP B and anti-Cy3 monoclonal antibody (Sigma-Aldrich, Steinheim, Germany).

2.2. Construction of the lateral flow biosensor

Rabbit anti-mouse polyclonal antibody (0.05 mg mL^{-1}, 50 µL, Abcam, Cambridge, USA) and SA (0.05 mg mL^{-1}, 50 µL, Sigma-Aldrich, Steinheim, Germany) were respectively dispensed onto
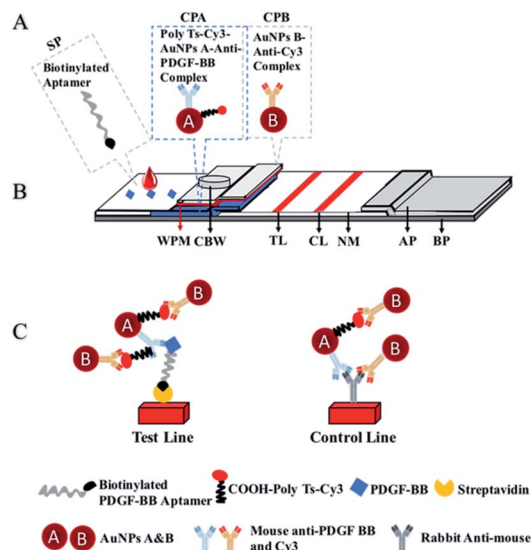

Fig. 1 Schematic illustration of the highly sensitive lateral flow biosensor (LFA). (A) The biotinylated aptamer was immobilized on the sample pad, while COOH-poly Ts-Cy3-AuNP A anti-PDGF BB complex and AuNP B-anti-Cy3 complex were immobilized to both conjugate pads (CPA/CPB), respectively. (B) The complexes were assembled to the biosensor's nitrocellulose membrane (NM) containing streptavidin on the test line (TL) and rabbit anti-mouse on the control line (CL). (C) Upon PDGF BB recognition by the aptamer, the target-aptamer complex flow and react with CPA's Mouse anti-PDGF BB, which is subsequently captured by mouse anti-Cy3. The AuNPs' complex is captured on the TL zone by the immobilized streptavidin, and excessive complexes are captured on the CL by the rabbit anti-mouse. Other parts of the proposed biosensor: waterproof membrane (WPM), chasing buffer well (CBW), absorbent pad (AP), backing pad (BP).

a 25 mm wide strip of nitrocellulose membrane (Shantou Ealon, Shantou, China) to form control and test zones, respectively, using a lateral flow dispenser (Shanghai Kinbio, Shanghai, China). The membrane was then dried at 50 °C for 12 hours and kept in low humidity room (<30%) or dessicant containing plastic bags.

Fiberglass (Shanghai Kinbio, Shanghai, China) strips of 25 mm in width were soaked in sample pad buffer (1% Triton, 1% BSA, 2% glucose, 50 mM biotinylated aptamer, 100 µM of biotinylated aptamer, pH 8.0). Then, the sample pads were dried and stored in the low humidity room at 25 °C.

The polyT-Cy3-AuNP A-anti-PDGF-BB complexes (2.2 µL cm^{-1}) were dispensed onto a 7 mm wide strip of fiberglass to form conjugate pad A. The AuNP B-anti-Cy3 complexes (2.2 µL cm^{-1}) were dispensed onto a strip of fiberglass (15 mm in

Table 1 Poly Ts oligonucleotides

Name	Sequences (5'–3')
Biotinylated aptamer	AGGGGCGCGTTCTTCGTGGTTACTTTTAGTCCCGTTTTTT-biotin
COOH-poly Ts1-Cy3	COOH-TTTTTTTTTTTTTTTTT-Cy3
COOH-poly Ts2-Cy3	COOH-TTTTTTTTTTTTTTTTTTTTTTTTTTTTTTT-Cy3
COOH-poly Ts3-Cy3	COOH-TTTTTTTTTTTTTTTTTTTTTTTTTTTTTTTTTTTTTTTT TTTTT-Cy3
COOH-poly T4-Cy3	COOH-TTTTTTTTTTTTTTTTTTTTTTTTTTTTTTTTTTTTTTTTTTTTTTTTTTTTTTTTTTTT-Cy3
COOH-poly Ts5-Cy3	COOH-TTTTTTTTTTTTTTTTTTTTTTTTTTTTTTTTTTTTTTTTTTTTTTTTTTTTTTTTTTTTTTTTTTTTTTTTTTTTTTTT-Cy3

width) to form conjugate pad B. Conjugate pads A and B were then dried at 50 °C for 12 h and kept at low humidity.

The absorbent pads (Shanghai Kinbio, Shanghai, China) were strips of thick absorbent paper 17 mm in width. Water-proof membranes were strips 20 mm in width. Our biosensor was then assembled using the conjugate pad B, waterproof membrane, sample pad, conjugate pad A, nitrocellulose membrane and absorbent pad were attached along the long axis of an adhesive plate with an overlap of 2–3 mm in the order shown in Fig. 1B. The plate was then cut into 4 mm wide strips by a programmed high speed paper cutter (Shanghai Kinbio, Shanghai, China).

2.3. Detection of PDGF-BB protein

Twenty µL of different concentrations of purified PDGF-BB proteins (Abcam, Cambridge, USA), breast cancer serum and PDGF-BB spiked serum (10%) were directly loaded to sample pad. Then, a loading buffer for signal enhancement, 1.5 µL of AuNP B–Anti Cy3 complexes and 40 µL of loading buffer (20 mM Tris–HCl, 150 mM NaCl, pH 8.0) was loaded up to the final volume of 60 µL were subsequently loaded in conjugate pad B 5 minutes later. For semi-quantification, the biosensor was then scanned after 5 minutes using a handheld "strip reader" (Shanghai Kinbio, Shanghai, China). PDGF-AA, PDGF-AB, and Epidermal Growth Factor (EGF) were bought from Abcam (Cambridge, USA). The human serum samples were bought from Xinfan (Shanghai, china). The LFA was read using a portable LFA reader (Shanghai Kinbio, Shanghai, China) and peak areas were obtained using ImageJ (NIH, USA), which provided peak intensity values to plot test lines colorimetric signal intensities.

2.4. Statistical analysis

Results are expressed as means $\pm$ SD. Data were analyzed using SPSS 11.0 Software (SPSS Inc., IL., US). A P-value less than 0.05 was regarded to be statistically significant.

3. Results and discussion

3.1. Working principle of the proposed biosensor

In this study, we first report a highly sensitive biosensor for PDGF-BB with an enhanced signal at the test line by using two different gold nanoparticles (AuNPs). The biosensor includes six components: a sample pad, a nitrocellulose membrane, an absorbent pad and two conjugate pads separated by a water-proof membrane (Fig. 1). One conjugate pad contains AuNPs A–anti-PDGF-BB complex modified with a 5′ carboxyl group and a 3′ Cy3 group on functionalized polythymine (Ts) oligonucleotides, while the other pad is composed of AuNP B-anti-Cy3 conjugate. Rabbit anti-mouse polyclonal antibody and SA were respectively fixed in the nitrocellulose membrane at the control and test zones. When the target PDGF-BB protein was added, it bound the biotinylated aptamer immobilized in the sample pad, and then captured at the first conjugate pad A to form poly Ts-Cy3-AuNP A-anti-PDGF-BB-aptamer-biotin complex. Next, the biotin on the complex was captured by SA to form a red line on the test zone. The excess complexes without PDGF-BB

protein continued to migrate towards the absorbent pad and were captured with the second antibody on the control line. To enhance the signal on the test line, we subsequently migrated the AuNP B-anti-Cy3 conjugate immobilized on conjugate pad B using to capture the Cy3-containing complexes on both the test and control zones. Due to the conjugation of AuNP A with different lengths of oligonucleotides which could increase the binding sites of the AuNP B-antibody complex.

The optical property of AuNPs enabled qualitative and semi-qualitative analysis of the test line by bare eye observation and optical density reading using a portable "strip reader", respectively. Thus, our biosensor performs without nuclease or fluorescence labeling and does not need complicated instruments to detect the target protein.

3.2. Optimization of parameter conditions

Concentrations of NaCl in the loading buffer and pH for the test condition were investigated in order to optimize the parameter conditions. The biosensor was tested in the presence of 30 ng mL^{-1} of the purified PDGF-BB protein loaded with different concentrations of NaCl in the loading buffer. Bands were observed at 150 mM NaCl (Fig. 2A), which were consistent with the calculated peak areas (Fig. 2B).

3.3. Sensitivity of the biosensor

Different concentrations of purified PDGF-BB protein were used to test the sensitivity of the proposed biosensor. Fig. 3A shows
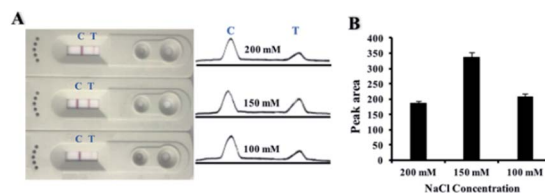

Fig. 2 (A) Biosensor loaded with the corresponding intensities in the presence of different concentrations of NaCl: 100 mM, 150 mM, 200 mM in loading buffer. (B) Comparison of test line peak areas responding to different concentrations of NaCl in loading buffer (*p < 0.05, n = 3).
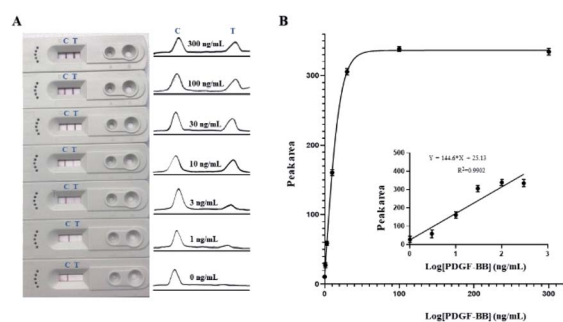

Fig. 3 (A) Illustration of the LFA detection response (left) and the corresponding semi-quantitation intensities (right) loaded with 0, 1, 3, 30, 100 and 300 ng mL^{-1} of purified PDGF-BB protein. (B) Comparison of peak areas of the test lines corresponding to different concentrations of PDGF-BB (*p < 0.05, n = 3).

Table 2 Comparison of different PDGF-BB detection methods

Method	Detection range (ng mL^{-1})	LOD (ng mL^{-1})	Reference
An AuNPs colorimetric sensor with isothermal strand displacement amplification	37–1480	20.38	33
An aptasensor with graphene oxide fluorescence resonance energy transfer	3.0895–21.5895	3.0895	34
A hydroxylamine amplified gold nanoparticle-based aptasensor	1.11–111	1.11	35
A fluorescence aptasensor based on silver nanoparticles	10–100	7	36
A fluorescent aptasensor based on split complementary strand of aptamer and magnetic beads	3.7–1850	2.405	37
A colorimetric assay integrated polymerase-mediated rolling-circle amplification and DNA enzyme-catalyzed colorimetric reaction	0.0007585–0.07585	0.000151 7	38
A fluorescence assay on a functionalized diamond surface	0.074–1850	0.074	39
Electrochemiluminescence assay	1.85–1.85 × 10^7	1.48	40
A signal-enhanced and sensitive LFA for the rapid detection of PDGF-BB	3–300	1	This study

the biosensor detection response and the corresponding semi-quantitation when loaded with different concentrations from 0, 1, 3, 10, 30, 100 to 300 ng mL^{-1} of the PDGF-BB protein. No band was observed in the absence of PDGF-BB at the test zone. The semi-quantitation results showed a visible line at the test zone as low as 1 ng mL^{-1} and of PDGF-BB protein, which can be deemed as the threshold for visual detection (Fig. 3A). This sensitivity was obtained in 10 minutes. The intensities of the bands increased gradually with the concentration of PDGF-BB at the test zones (Fig. 3B). The regression equation is $Y = 144.6X + 25.13$ with a correlation coefficient of 0.9902, where Y is peak area of the test line, and X is the log concentration of PDGF-BB. This enhanced response provided several advantages over previously published methods (Table 2),[33–40] and was 1000 times smaller than the traditional double sandwich antibody lateral flow biosensor (Fig. 6).

Moreover, this approach takes less time and implies a novel method for the rapid detection of cell factors. Such activity can be attributed to the combination of PDGF-BB protein recognition elements (aptamer and monoclonal antibody) as well as our novel test line signal enhancement *via* the dual conjugate pads. This activity could be associated with the amino groups on the AuNP A reacting with the carboxyl groups on the poly Ts oligonucleotides, which increased the binding sites of AuNP B-anti-Cy3 complex and later binding on the test line complex. This method could also be used as an alternative for apparatus-based assays to simplify the detection process, thereby displaying results through red lines readable by the naked eye.

The performance of our biosensor was further verified by the conventional ELISA method, which achieved the detection range approximately 1–50 pg mL^{-1} (Fig. 7). Although the biosensor was less sensitive than ELISA, our method was much

faster, easier and inexpensive than ELISA or other methods for PDGF-BB detection.[15–18]

3.4. Specificity of the biosensor

The specificity was tested using optimized loading buffer for molecular interactions prior to testing various interfering closely and non-closely related components (proteins, DNAs, *etc.*). As shown in Fig. 4A, the biosensor exhibited a test test line responses in the presence of 100 ng mL^{-1} purified PDGF-BB but not in other non-specific components. The quantitative measurements and peak area results also confirmed this activity (Fig. 4B), validating the excellent performance of this biosensor.

The specificity of the biosensor was further examined by substituting the PDGF-BB recognizing aptamer with a nonspecific biotinylated oligonucleotide (Table 1, Shanghai Sangon Biological Engineering Technology, Shanghai, China) on the
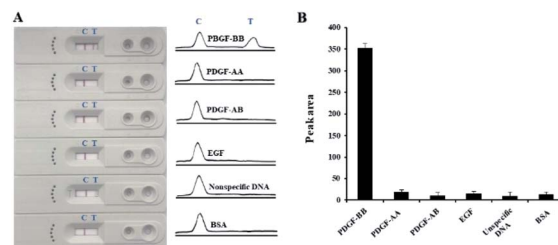

Fig. 4 (A) LFA (left) and its corresponding semi-quantitation (right) loaded concentrations with PDGF-BB protein, PDGF-AA protein, PDGF-AB protein, EGF protein, a nonspecific oligonucleotide, and BSA protein. (B) Comparison of test line peak areas corresponding to PDGF-BB protein, PDGF-AA protein, PDGF-AB protein, EGF protein, a nonspecific oligonucleotide, and BSA protein (*$p < 0.05$, $n = 3$).

Table 3 Recovery of PDGF-BB added into serum samples

Added amount ($ng\ mL^{-1}$)	Measured amount ($ng\ mL^{-1}$)	Recovery (%)	RSD (%)
3	2.91	97	4.5
30	31.4	104.7	3.8
100	102.9	102.9	4.1

sample pad, and a new biosensor was constructed using a new sample pad buffer (1% Triton, 1% BSA, 2% glucose, 50 mM boric acid, 100 μM nonspecific biotinylated oligonucleotide, pH 8.0). As shown in Fig. 4, only the biosensors with the original binding aptamer sequence exhibited observable red color on the test line. These results show that the biosensor has high sensitivity and specificity and enhances the signal of the test line. This effect could be attributed to the integrated system containing the following: (1) monoclonal antibody against PDGF-BB captured by AuNP A; (2) the amino groups on the monoclonal antibody (against PDGF-BB and BSA) binding to AuNP A, which reacts with the carboxyl groups on oligonucleotides; (3) PDGF-BB protein recognizing aptamer in the sample pad; and (4) AuNP B-antibody against Cy3 complexes captured by the Cy3 of AuNP A-poly Ts-Cy3-Anti-PDGF-BB-aptamer-biotin-SA complex on the test zone.

The assay displays selectivity with no background, which has several advantages over other previously published methods.[6,18,19] First, the amino groups on the monoclonal antibody against PDGF-BB and BSA binding to AuNP A react with the carboxyl groups on oligonucleotides, which increases the binding sites of the AuNP B-antibody complex. Second, the sample pad buffer contains the aptamer which lengthened the reaction time of the aptamer and PDGF-BB protein.

3.5. Analysis of clinical samples

To investigate the practicality of the biosensor, different concentrations of PDGF-BB were spiked into human serum samples and the method was applied to detect clinical samples. As shown in Table 3, the recovery efficiency of the aptasensor ranged from 97 to 102.9%. These results confirmed that the lateral flow aptasensor is practical for detection of PDGF-BB in clinical samples without the interference of other substances in serum samples.

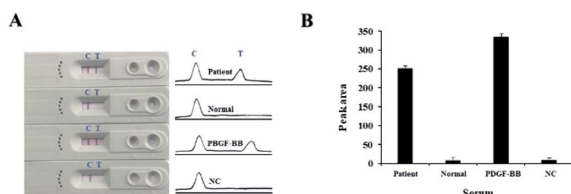We next tested 6 breast cancer negative and positive, and controls (PGDF-BB, loading buffer) samples. As the lower detection limit of our present method was 3 ng mL^{-1} with a good linear range to 100 ng mL^{-1}, the clinical serum samples from breast cancer patients showed a visible red line at the test lines (Fig. 5A). No observable red band was observed in samples from normal people. The PDGF-BB protein in the same samples was proportional to the quantitative measurements and peak areas from breast cancer patients compared to normal people (Fig. 5B). The detectable noise in normal samples could be explained that the mean PDGF-BB concentration in normal samples has been found to be 0.32 ± 0.4 ng mL^{-1}.[41]

4. Conclusion

In conclusion, we have developed a novel highly sensitive biosensor for PDGF-BB detection with enhanced signal intensity at the test line as a result of dual conjugate pads. It successfully achieved a sensible linear range up to 100 ng mL^{-1} for PDGF-BB cancer biomarker in 10 minutes of naked eyes readable red lines. In addition, our produced sample pad buffer lengthened the reaction time of the aptamer with PDGF-BB protein, thus excluding the need of sample pre-treatment. Moreover, the biosensor retained high specificity in the presence of various interfering compounds and proved applicability for clinical sample. Apart from singleplex, multiplex detection of other biomarker(s) by substitution of target recognition molecule(s) and tuning of buffer. Therefore, it is noteworthy mentioning that this biosensor promises PDGF-BB based cancer prognosis and monitoring.

Appendices

Construction of the traditional antibody double sandwich gold detection method for PDGF-BB protein

The traditional antibody double sandwich gold detection method for PDGF-BB protein was mainly constructed with a sample pad, a conjugate pad, a strip of nitrocellulose membrane, and an absorbent pad. The monoclonal antibody
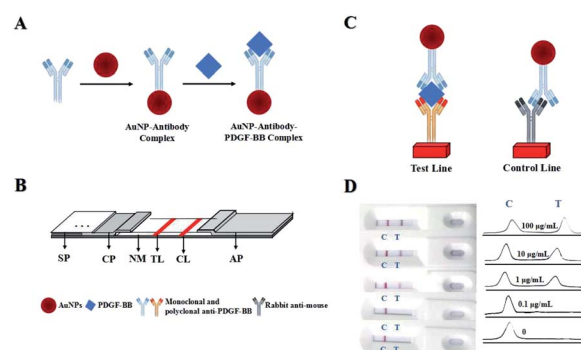

Fig. 5 (A) Representative LFA picture (left) and corresponding semi-quantitation (right) of the assay loaded with clinical sera and negative controls. (B) Comparison of test line peak areas corresponding to clinical serum and negative control (*$p < 0.05$, $n = 3$).

Fig. 6 The traditional antibody double sandwich gold nanoparticles detection method for PDGF-BB protein. (A) The monoclonal antibody against PDGF-BB binds to the gold nanoparticles. (B) Schematic of the biosensor. (C) PDGF-BB protein and excessive sample pad complexes are respectively captured on the test and control lines. (D) Results with the traditional antibody double sandwich gold nanoparticles detection method. Sample pad (SP), conjugate pad (CP), nitrocellulose membrane (NM), test line (TL), control line (CL), absorbent pad (AP).
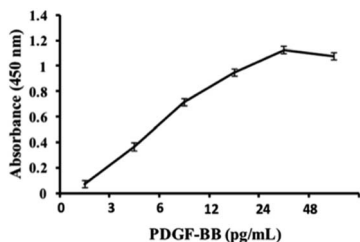
Fig. 7 ELISA sensitivity for purified PDGF-BB protein (*$p < 0.05$, $n = 3$).

against PDGF-BB was coated with 40 nm AuNPs. Both polyclonal antibody against PDGF-BB and the rabbit anti-mouse polyclonal antibody were respectively loaded onto the nitrocellulose membrane at the test and control zones. The PDGF-BB protein bound the monoclonal antibody to form AuNP-antibody complexes. The PDGF-BB protein was captured by the polyclonal antibody to form a clear red test line. The unbound complexes continued to migrate towards the absorbent pad and were captured by the rabbit anti-mouse polyclonal antibody on the control zone (Fig. 6A–C). As shown in Fig. 7D, the detection limit was 1 µg mL^{-1}.

ELISA for PDGF-BB protein

Different concentrations of PDGF-BB protein samples were confirmed by the conventional ELISA method (Fig. 7).

Conflicts of interest

There are no conflicts to declare.

Acknowledgements

References

1 A. Csordas, A. E. Gerdon, J. D. Adams, J. Qian, S. S. Oh, Y. Xiao and H. T. Soh, *Angew. Chem.*, 2010, **49**, 355–358.

2 D. A. Bronzert, P. Pantazis, H. N. Antoniades, A. Kasid, N. Davidson, R. B. Dickson and M. E. Lippman, *Proc. Natl. Acad. Sci. U.S.A.*, 1987, **84**, 5763–5767.

3 D. F. Bowen-Pope, T. W. Malpass, D. M. Foster and R. Ross, *Blood*, 1984, **64**, 458–469.

4 K. Leitzel, W. Bryce, J. Tomita, G. Manderino, I. Tribby, A. Thomason, M. Billingsley, E. Podczaski, H. Harvey and M. Bartholomew, *Cancer Res.*, 1991, **51**, 4149–4154.

5 F. Qu, H. Lu, M. Yang and C. Deng, *Biosens. Bioelectron.*, 2011, **26**, 4810–4814.

6 Z. Jing, Z. Min, X. Guo, J. Wang and J. Xu, *Sens. Actuators, B*, 2017, 250.

7 M. Mascini, I. Palchetti and S. Tombelli, *Angew. Chem.*, 2012, **51**, 1316–1332.

8 X. Ouyang, R. Yu, J. Jin, J. Li, R. Yang, W. Tan and J. Yuan, *Anal. Chem.*, 2011, **83**, 782–789.

9 F. Chen, Y. Liu, C. Chen, H. Gong, C. Cai and X. Chen, *Sens. Actuators, B*, 2017, **245**, 470–476.

10 A. Qureshi, Y. Gurbuz and J. H. Niazi, *Sens. Actuators, B*, 2015, **220**, 1145–1151.

11 Z. Zhu, C. Wu, H. Liu, Y. Zou, X. Zhang, H. Kang, C. J. Yang and W. Tan, *Angew. Chem.*, 2010, **49**, 1052–1056.

12 L. Yang, C. Fu, H. Wang, S. Xu and W. Xu, *Anal. Bioanal. Chem.*, 2017, **409**, 235–242.

13 B. Wu, R. Jiang, Q. Wang, J. Huang, X. Yang, K. Wang, W. Li, N. Chen and Q. Li, *Chem. Commun.*, 2016, **52**, 3568–3571.

14 W. Dong, Y. Li, D. Niu, Z. Ma, J. Gu, Y. Chen, W. Zhao, X. Liu, C. Liu and J. Shi, *Adv. Mater.*, 2011, **23**, 5392–5397.

15 X. Wang, Y. Ishii, A. R. Ruslinda, M. Hasegawa and H. Kawarada, *ACS Appl. Mater. Interfaces*, 2012, **4**, 3526–3534.

16 A. R. Ruslinda, S. Tajima, Y. Ishii, Y. Ishiyama, R. Edgington and H. Kawarada, *Biosens. Bioelectron.*, 2011, **26**, 1599–1604.

17 E. Babu, S. Singaravadivel, P. Manojkumar, S. Krishnasamy, G. Gnana kumar and S. Rajagopal, *Anal. Bioanal. Chem.*, 2013, **405**, 6891–6895.

18 X. Jin, J. Zhao, L. Zhang, Y. Huang and S. Zhao, *RSC Adv.*, 2014, **4**, 6850.

19 C. Wickenhauser, A. Hillienhof, K. Jungheim, J. Lorenzen, H. Ruskowski, M. L. Hansmann, J. Thiele and R. Fischer, *Leukemia*, 1995, **9**, 310–315.

20 Z. Zhang, C. Guo, S. Zhang, L. He, M. Wang, D. Peng, J. Tian and S. Fang, *Biosens. Bioelectron.*, 2017, **89**, 735–742.

21 H. Zhang, X. F. Li and X. C. Le, *Anal Chem.*, 2009, **81**, 7795–7800.

22 K. L. Hong and L. J. Sooter, *BioMed Res. Int.*, 2015, **419318**, 1–31.

23 K. Ikebukuro, Y. Okumura, K. Sumikura and I. Karube, *Nucleic Acids Res.*, 2005, **33**, e108.

24 D. M. Kolpashchikov and M. N. Stojanovic, *J. Am. Chem. Soc.*, 2005, **127**, 11348–11351.

25 Y. Lin and S. D. Jayasena, *J. Mol. Biol.*, 1997, **271**, 100–111.

26 L. X. Fang, K.-J. Huang and Y. Liu, *Biosens. Bioelectron.*, 2015, **71**, 171–178.

27 L. Rivas, C. C. Mayorga-Martinez, D. Quesada-Gonzalez, A. Zamora-Galvez, A. de la Escosura-Muniz and A. Merkoci, *Anal. Chem.*, 2015, **87**, 5167–5172.

28 Z. Zhang, C. Tao, J. Yin, Y. Wang and Y. Li, *Biosens. Bioelectron.*, 2018, **103**, 39–44.

29 G. Liu, A. S. Gurung and W. Qiu, *Molecules*, 2019, **24**, 756–767.

30 Z. Y. Fang, C. C. Ge, W. Zhang, P. C. Lie and L. W. Zeng, *Bioelectron*, 2011, **1**, 192–196.

31 J. Jun, J. S. Lee, D. H. Shin and J. Jang, *ACS Appl. Mater. Interfaces*, 2014, **6**, 13859–13865.

32 S. Gao, X. Zheng and J. Wu, *Biosens. Bioelectron.*, 2018, **102**, 57–62.

33 H. Zhang, F. Li, H. Chen, Y. Ma, S. Qi, X. Chen and L. Zhou, *Sens. Actuators, B*, 2015, **207**, 1692–1697.

34 J. Liang, R. Wei, S. He, Y. Liu, L. Guo and L. Li, *Analyst*, 2013, **138**, 1726.

35 P. Wang, Y. Song, Y. Zhao and A. Fan, *Talanta*, 2015, **103**, 392–397.

36 X. Wang, W. Li, Z. Li, H. Li and D. Xu, *Talanta*, 2015, **144**, 1273–1278.

37 A. Bahreyni, S. Tahmasebi, M. Ramezani, M. Alibolandi, N. Danesh, K. Abnous and S. Taghdisi, *Sens. Actuators, B*, 2019, **280**, 10–15.

38 L. Tang, Y. Liu, M. M. Ali, D. K. Kang, W. Zhao and J. Li, *Anal. Chem.*, 2013, **84**, 4711–4717.

39 A. R. Ruslinda, V. Penmatsa, Y. Ishii, S. Tajima and H. Kawarada, *Analyst*, 2013, **137**, 1692.

40 D. Zhu, X. Zhou and D. Xing, *Biosens. Bioelectron.*, 2010, **26**, 285–288.

41 K. Leitzel, W. Bryce, J. Tomita, G. Manderino and M. Bartholomew, *Cancer Res.*, 1991, **51**, 4149–4154.